

# Relationship between MRA-derived pattern of artery occlusion and MRI-based tissue diffusion and perfusion lesion in a rat embolic stroke model

Mark J Bouts<sup>1</sup>, Ivo A Tiebosch<sup>1</sup>, Annette van der Toorn<sup>1</sup>, Jeroen Hendrikse<sup>2</sup>, and Rick M Dijkhuizen<sup>1</sup>

<sup>1</sup>Biomedical MR Imaging and Spectroscopy Group, Image Sciences Institute, University Medical Center Utrecht, Utrecht, Utrecht, Netherlands, <sup>2</sup>Radiology, University Medical Center Utrecht, Utrecht, Utrecht, Netherlands

## Introduction

Early assessment of cerebrovascular impairment and prediction of outcome is crucial for adequate management and treatment of patients suffering from acute, ischemic stroke. A major factor in the development of an ischemic lesion is the location and extent of cerebral vessel occlusion. It has therefore been speculated that angiography-based detection of the site of cerebral vessel occlusion can significantly aid in early diagnosis and treatment planning [1, 2]. However, the relationship between the spatiotemporal pattern of ischemic brain lesion development and the extent of occlusion in brain supplying arteries is largely unclear. Therefore we aimed to characterize and correlate the pattern of occlusion of segments of the Circle of Willis, as measured with MRA, and acute ischemic lesions, as measured with diffusion- and perfusion-weighted MRI, in a rat embolic stroke model.

## Materials & Methods

MRI data of 51 male Wistar rats were analyzed from an ongoing treatment study after experimental ischemic stroke. All animal procedures were approved by our institution's animal welfare and care committee. Animals were subjected to occlusion of the right middle cerebral artery (MCA) by injection of an autologous blood clot. MRI was executed in the first hours after stroke induction. Diffusion-weighted MRI (spin echo eight-shot EPI; TR=3000ms; TE=38.5ms; b=0 and 1430 s/mm<sup>2</sup>; FOV=32x32x19mm<sup>3</sup>; 128x128x19 data matrix), dynamic susceptibility contrast-enhanced (DSC) MRI gradient echo EPI;  $\alpha=35^\circ$ ; TR=330 ms; TE=25 ms; FOV=32x32x9mm<sup>3</sup>; 64x64x5 data matrix), and 3D time-of-flight MRA (gradient echo; TR=15 ms; TE=2.66 ms; FOV=32x32x32mm<sup>3</sup>; 128x128x128 data matrix) were conducted on a 4.7T horizontal bore MR spectrometer (Agilent, Palo Alto, CA, USA). Quantitative maps of the trace of the apparent diffusion coefficient (ADC<sub>trace</sub>), cerebral blood flow index (CBFi), cerebral blood volume (CBV), mean transit time (MTT), and tracer arrival delay were calculated from the acquired data. Parametric maps were spatially aligned to a common rat brain template. Abnormal tissue water diffusion was identified as a deviation of more than 2 $\sigma$  from mean contralateral ADC values in four consecutive slices. A similar approach was used for identifying perfusion abnormality on MTT maps. Vessel occlusion sites were identified by visual assessment of vessel status on MR angiograms. Occlusions of the internal carotid artery (ICA) and the proximal (M1) and distal (M2) segments of the MCA were categorized in seven different types. Table 1 shows the pattern of occlusions, where '1' and '0' reflect open artery and closed arteries, respectively. Animals were grouped according to ICA/MCA occlusion pattern, and voxel-wise lesion incidence maps were made to assess the extent of diffusion and perfusion abnormality. Statistical differences were determined using Fisher's exact test for the categorical data and Kruskal-Wallis with post hoc Wilcoxon rank-sum test for continuous data. False discovery rate measurement was used for compensation of multiple comparisons. P<0.05 was considered significant.

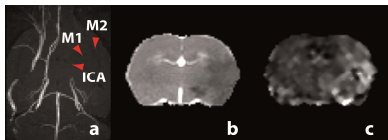


**Figure 1.** Post-stroke MIP (a), ADC map (b), and MTT map (c) of a rat with occlusion of the ICA and MCA (arrowheads).

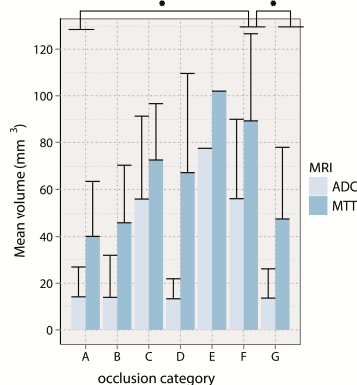


**Figure 3:** Mean brain tissue volume (mm<sup>3</sup>) with abnormal ADC and MTT for the different occlusion categories (\*p<0.05).

incomplete occlusions of both MCA segments led to only subcortical lesions. This indicates that in rats areas supplied by the proximal segment of the MCA have less benefit from collateral circulation compared to occlusion of only the ICA, which is in correspondence with findings in stroke patients [2]. The combination of MRA-derived vessel occlusion pattern with diffusion- and perfusion-weighted MRI-based lesion mismatch assessment may lead to more reliable outcome prediction and more favorable treatment planning after acute stroke.

**References:** [1] Lee LJ, et al. *Stroke*.31:1081-9 (2000). [2] Lansberg MG, et al. *Stroke*: 39:2491-96.

Group	ICA	MCA.M1	MCA.M2	Incidence %-age
A	1	1	1	35
B	1	1	0	14
C	1	0	0	4
D	0	1	0	8
E	0	0	1	2
F	0	0	0	22
G	0	1	1	15

Table 1: Type and incidence of ICA/MCA occlusion patterns.

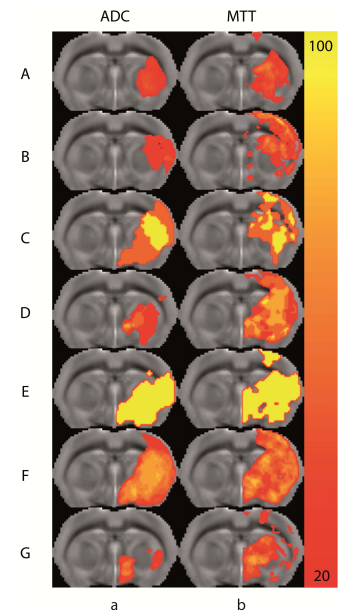


**Figure 2.** Diffusion- (a) and perfusion-based lesion incidence maps (b) of seven occlusion groups, overlaid on a single slice from rat brain template. (incidence from 20-100%)

**Results** Table 1 shows the incidence of different occlusion patterns. The largest groups consisted of animals with no clear occlusion in the ICA or MCA (Group A; 35%), and animals with occlusion in all segments of the right ICA and MCA (Group F; 22%). Other animals had varying profiles of occlusion of parts of the ICA and MCA. Figure 1a shows a transversal maximum intensity projection (MIP) of a Group F rat, depicting occlusion of the right ICA, MCA.M1 and MCA.M2 (arrowheads). Resultant acute brain lesions were evident on ADC<sub>trace</sub> (b) and MTT (c) maps showing the tissue area with diffusion (ADC reduction) and perfusion abnormality (MTT prolongation). Figure 2 shows the incidence maps of abnormal diffusion (a) and perfusion (b) for all groups. Groups with MCA.M1 occlusions, i.e. C, E and F, had the largest lesions with involvement of substantial parts of the ipsilateral cortex and striatum, i.e. the territory supplied by the MCA. Groups A and G, without evident MCA occlusion, showed the smallest lesions in predominantly subcortical areas. In all groups, acute perfusion lesions were larger than tissue diffusion lesions. Figure 3 shows the mean diffusion and perfusion volumes for the different occlusion patterns. Occlusion of the MCA.M1 (C, E and F) resulted in the largest lesions, where Group F lesion volumes were significantly larger than those in Groups A (p=0.001) and G (p=0.04), which showed no clear MCA occlusion. Mismatch between the volumes of acute diffusion and perfusion abnormalities significantly differed in Groups A (mean mismatch volume: 26±22 mm<sup>3</sup>; p=0.0002), B (31±13 mm<sup>3</sup>; p=0.02), F (33±38 mm<sup>3</sup>; p=0.03) and G (34±23 mm<sup>3</sup>; p=0.01). Statistical significance was absent in Groups D (53±40 mm<sup>3</sup>; p=0.1), C (17±11 mm<sup>3</sup>; p=0.37) and E (24 mm<sup>3</sup>).

## Discussion

In this study we investigated the relationship between vessel occlusion sites and acute brain tissue diffusion and perfusion lesion locations after experimental embolic stroke in rats. The site of occlusion strongly influenced the distribution of diffusion and perfusion abnormalities. Occlusion of the M1 segment of the MCA, in combination with an open or closed MCA.M2 and/or ICA, resulted in ischemic lesions in major part of the MCA-supplied territory. Whereas incomplete occlusions of both MCA segments led to only subcortical lesions. This indicates that in rats areas supplied by the proximal segment of the MCA have less benefit from collateral circulation compared to occlusion of only the ICA, which is in correspondence with findings in stroke patients [2]. The combination of MRA-derived vessel occlusion pattern with diffusion- and perfusion-weighted MRI-based lesion mismatch assessment may lead to more reliable outcome prediction and more favorable treatment planning after acute stroke.